Glass Transition Behavior Including Retrograde Vitrification of Polymers with Compressed Fluid Diluents†

P. D. Condo, I. C. Sanchez,* C. G. Panayiotou,‡ and K. P. Johnston*

Department of Chemical Engineering, The University of Texas at Austin, Austin, Texas 78712

Received March 16, 1992; Revised Manuscript Received June 24, 1992

ABSTRACT: A model is presented to predict the depression of the glass transition temperature of a polymer in the presence of a liquid, gas, or supercritical fluid as a function of pressure. It is developed using lattice fluid theory and the Gibbs–Di Marzio criterion, which states that the entropy is zero at the glass transition. Four fundamental types of T_g versus pressure behavior are identified and interpreted as a function of three factors: the solubility of the compressed fluid in the polymer, the flexibility of the polymer molecule, and the critical temperature of the pure fluid. A new phenomenon is predicted where a liquid to glass transition occurs with increasing temperature, which we define as retrograde vitrification. This retrograde behavior is a consequence of the complex effects of temperature and pressure on sorption. For the limited data which are available for the polystyrene–CO_2 and poly(methyl methacrylate)–CO_2 systems, the predictions of the model are in good agreement with experiment.

Introduction

A broad range of applications have been proposed for processing polymers with compressed fluids, including supercritical fluids.[1-5] These fluids may be used to purify polymers by extracting monomers, solvent, and oligomers,[6-8] to concentrate polymer solutions by facilitating lower critical solution temperature phase separation,[2,9] and to fractionate polymers.[10-12] They may also be used to plasticize polymers,[13-18] to reduce the viscosity of polymer melts and solutions,[19] to condition polymeric membranes,[20] and to produce microcellular foams,[21] microspheres,[22-25] and fibers.[26-29] Recently, an environmentally acceptable process has been commercialized for spray painting and coating with polymers by using CO_2 as the diluent replacing alkane solvents.[30,31]

There are a number of advantages of polymer processing with compressed and supercritical fluids, despite the need for elevated pressures. For example, CO_2 is a small, linear molecule; thus sorption and desorption are far more rapid than for larger liquid solvents. Unlike the case for a liquid or polymeric diluent, the sorption of a compressed fluid diluent may be adjusted readily over a continuum with pressure and temperature. After depressurization, the solvent residue in the polymer is far less, and CO_2 is more environmentally acceptable.

In most of the above applications, the (desired or undesired) effect of dissolved fluids on the morphology of the polymer plays a central role. Since the sorption of a compressed fluid in a polymer is adjustable, the polymer morphology may be tailored with modest changes in temperature and pressure. In this study, we concentrate on the depression of the glass transition temperature of a polymer as a function of the sorption of the fluid.

Interesting observations have been made regarding the influence of a compressed fluid on the glass transition temperature of a polymer. Assink[32] showed that a compressed fluid with a low solubility will act strictly as a pressure-generating medium, thus increasing the T_g with increasing pressure, while a more soluble fluid may effectively plasticize a polymer and decrease T_g. Wang et al.[13] proposed that a single compressed fluid may produce both effects leading to a T_g minimum. Recently, significant depressions of the glass transition temperature have been observed due to high levels of dissolution of compressed fluids.[14-16] The largest T_g depression claimed as of this writing is 227 °C![15]

The calculation of the T_g depression caused by a compressed fluid has been performed with a lattice fluid model.[14,16] Since this particular model was originally developed for liquid plasticizers,[33] it does not consider pressure explicitly as an independent variable. The diluent concentration was treated as an independent variable, and the equilibrium partitioning of the diluent was not addressed. The Gibbs–Di Marzio criterion of the glass transition was used.[34,35] The effectiveness of the model has been shown to be restricted to systems with low solubility levels of the compressed fluid in the polymer.[16]

Recent lattice models are more general, since they treat temperature and pressure as the independent variables and also address the phase behavior. These newer models differ from each other with regard to the definition and application of the glass transition criterion. Each model requires some equilibrium data, e.g., sorption data, to describe the interaction between the fluid and polymer. Beckman's study considers separately three criteria for the glass transition: the free volume, mixture entropy, and temperature–entropy product.[36,37] The model predicts T_g minimum data[13] successfully with the temperature–entropy product criterion. In another approach, Wissinger and Paulaitis[38] measured T_g depressions which were correlated with a free volume parameter. This model relates T_g and sorption successfully but requires experimental T_g data, limiting the predictive ability of the model. Kalospiros, Astarita, and Paulaitis[39] applied order parameter theory to relate the T_g of the polymer to the solubility of the compressed fluid. The free volume order parameter is variable in the glassy region, providing a more physical description of the system than in an earlier model.[38] To calculate this order parameter, it is necessary to have specific volume data for the pure glassy polymer over the temperature range of interest. The model predicts T_g quite well as a function of the sorption of the compressed fluid in the polymer but did not examine the T_g behavior versus pressure.

Our objective is to develop a model to predict the T_g depression of a polymer caused by dissolution of a compressed fluid, which is sufficiently robust that only a

† This paper was presented at the American Institute of Chemical Engineers annual meeting in Los Angeles, CA, on Nov 19, 1991.

‡ On leave of absence from the Department of Chemical Engineering, University of Thessaloniki, 54006 Thessaloniki, Greece.

0024-9297/92/2225-6119$03.00/0

minimal amount of data are required. The model combines lattice fluid theory[40-44] and the Gibbs–Di Marzio criterion of the glass transition[34,35] in a consistent framework. It is a significant advancement in that the only required information about the nature of the glassy polymer is the normal T_g at atmospheric pressure and the dT_g/dP behavior of the pure polymer. New regimes in temperature, pressure, and also the solubility of the fluid in the polymer, polymer flexibility, and critical temperature of the fluid are explored to identify and classify fundamental types of T_g versus pressure behavior. The model reveals a previously unknown phenomenon, where a polymer undergoes a liquid to glass transition with an increase in temperature, which we call retrograde vitrification. While the first part of the paper presents a general description of the fundamental types of T_g behavior, the second part compares predictions with a small amount of available experimental data for the poly(methyl methacrylate)–CO_2 and polystyrene–CO_2 systems.[14,16]

Theory

We wish to calculate the lattice free energy of a system of N_1 semiflexible molecules each consisting of r_1 segments or "mers", N_2 semiflexible molecules each consisting of r_2 mers, and N_0 holes. This problem was originally considered by Gibbs and Di Marzio.[34,35] Their calculation was carried out in a mean-field approximation in what is often referred to as the "Huggins approximation". If the lattice coordination number z is large, these mean-field equations simplify considerably; the large-z limit of these equations is known as the "Flory approximation". In this latter approximation, the number of system configurations is given by[40]

$$\Omega(f_1,f_2,N_0) = \left(\frac{1}{1-\tilde{\rho}}\right)^{N_0}\left(\frac{(\delta_1/\omega_1)}{\phi_1\tilde{\rho}}\right)^{N_1}\left(\frac{(\delta_2/\omega_2)}{\phi_2\tilde{\rho}}\right)^{N_2} \quad (1)$$

where δ_i is the chain flexibility parameter[34,44,45] and ω_i is an attrition factor:[40]

$$\delta_i = z\left(\frac{z-2}{f_i}\right)^{(r_i-2)f_i}\left(\frac{1}{1-f_i}\right)^{(r_i-2)(1-f_i)}; \qquad \omega_i = 2e^{r_i-1}/r_i \quad (2)$$

δ_i is the number of internal configurations available to a semiflexible chain molecule of r_i-mers in free space when $f_i(r_i-2)$ bonds in a type i molecule are in "flexed" or high-energy states and $(1-f_i)(r_i-2)$ bonds are in a low-energy state (for example, gauche and trans states). In a completely filled lattice, δ_i is reduced by a factor of ω_i caused by inter- and intramolecular interference (excluded volume). The fraction of occupied sites (or the reduced density), $\tilde{\rho}$, is defined by

$$\tilde{\rho} = \frac{r_1N_1 + r_2N_2}{N_0 + r_1N_1 + r_2N_2} \equiv \frac{rN}{N_0 + rN} \quad (3)$$

where r, N, and ϕ_i have their usual definitions

$$N = N_1 + N_2; \qquad x_i = N_i/N; \qquad \phi_i = r_iN_i/rN \quad (4)$$

$$r = x_1r_1 + x_2r_2 \quad \text{or} \quad 1/r = \phi_1/r_1 + \phi_2/r_2 \quad (5)$$

The mean-field system energy E is a combination of inter- and intramolecular energies:

$$E = -rN\tilde{\rho}\epsilon^* + N_1(r_1-2)f_1\Delta\epsilon_1 + N_2(r_2-2)f_2\Delta\epsilon_2 \quad (6)$$

$\Delta\epsilon_i$ is the increase in intramolecular energy that accompanies the "flexing" of a bond in a type i chain molecule. We have assumed for simplicity that this is a two-state model ($z-2$ of high energy and 1 of low energy). The creation of a vacancy in component 1 requires an energy ϵ_{11}^* and the creation of a vacancy in component 2 requires an energy ϵ_{22}^*. The creation of a vacancy in a binary mixture of 1 and 2 requires an energy ϵ^*. In a mean-field approximation

$$\epsilon^* = \phi_1\epsilon_{11}^* + \phi_2\epsilon_{22}^* - \phi_1\phi_2kTX_{12} \quad (7)$$

$$X_{12} = (\epsilon_{11}^* + \epsilon_{22}^* - 2\epsilon_{12}^*)/kT \quad (8)$$

$$\epsilon_{12}^* = \zeta_{12}(\epsilon_{11}^*\epsilon_{22}^*)^{1/2} \quad (9)$$

The factor of $\tilde{\rho}$ arises in eq 6 because the total attractive energy is $-rN\epsilon^*$ in the absence of vacancies ($\tilde{\rho} = 1$) and $-rN\tilde{\rho}\epsilon^*$ when $\tilde{\rho}$ of the sites are occupied.

The equilibrium number of flexed bonds is determined by finding the maximum term in the canonical partition function $\Omega e^{-E/kT}$ to yield the familiar Boltzmann expression:

$$f_i = \frac{(z-2)\exp(-\Delta\epsilon_i/kT)}{1 + (z-2)\exp(-\Delta\epsilon_i/kT)} \quad (10)$$

Note that when $\Delta\epsilon_i = 0$, $f_i = (z-2)/(z-1)$ and $\delta_i = z(z-1)^{r_i-2}$ as it should for a completely flexible chain without excluded volume.

The system volume is given by

$$V = (N_0 + rN)v^* \equiv rNv^*/\tilde{\rho} \equiv rNv^*\tilde{v} \quad (11)$$

with

$$v^* = \phi_1v_1^* + \phi_2v_2^* \quad (12)$$

and where v_i^* is the characteristic mer volume of component i. A nonlinear relation for v^* can be invoked,[43] but, for simplicity, we avoid that generalization here.

The Gibbs free energy of the system is given by

$$G = -kT\ln\{\sum_{N_0=0}^{\infty}\Omega(T,N_0)\exp[-(E+PV)/kT]\} \quad (13)$$

where P is the pressure. The maximum term in the sum is determined by the condition

$$\frac{\partial}{\partial N_0}\left(\ln\Omega - \frac{E+PV}{kT}\right)_{T,P} = 0 \quad (14)$$

which yields the familiar lattice fluid equation of state:[40]

$$\tilde{\rho}^2 + \tilde{P} + \tilde{T}[\ln(1-\tilde{\rho}) + (1-1/r)\tilde{\rho}] = 0 \quad (15)$$

$\tilde{T}$ and $\tilde{P}$ are the reduced temperature and pressure, respectively. The reduced density $\tilde{\rho}$, defined by eq 3, also has a simple experimental interpretation: it equals the ratio of the experimental mass density ρ at a given T and P to the hypothetical mass density ρ^* at absolute zero ($\tilde{\rho} = 1$). The three equation of state parameters T^*, P^*, and ρ^*, which can be determined from experimental PVT data, completely characterize the pure components. The size parameter r is related to the molecular weight M by

$$r_i = M_i/\rho_iv_i^* = M_iP_i^*/r_i^*kT_i^* \quad (16)$$

The system entropy is given by[45]

$$S = k\ln\Omega \quad (17a)$$

or

$$-S/k = rN\left\{(\tilde{v}-1)\ln(1-\tilde{\rho}) + \frac{\ln\tilde{\rho}}{r} + \left(\frac{\phi_1}{r_1}\right)\ln\left(\frac{\phi_1}{r_1}\right) + \left(\frac{\phi_2}{r_2}\right)\ln\left(\frac{\phi_2}{r_2}\right) + 1 + \frac{\ln(2/z)-1}{r} + \left(\frac{\phi_1}{r_1}\right)(r_1-2)\left[\ln(1-f_1) - f_1\frac{\Delta\epsilon_1}{kT}\right] + \left(\frac{\phi_2}{r_2}\right)(r_2-2)\left[\ln(1-f_2) - f_2\frac{\Delta\epsilon_2}{kT}\right]\right\} \quad (17b)$$

In eq 13, equating the Gibbs free energy to the maximum term yields

$$G = E - TS + PV \quad (18a)$$

$$G = rN\left\{-\tilde{\rho}\epsilon^* + Pv^*\tilde{v} + kT\left[(\tilde{v}-1)\ln(1-\tilde{\rho}) + \frac{\ln\tilde{\rho}}{r}\right] + kT\left[\left(\frac{\phi_1}{r_1}\right)\ln\left(\frac{\phi_1}{r_1}\right) + \left(\frac{\phi_2}{r_2}\right)\ln\left(\frac{\phi_2}{r_2}\right) + 1 + \frac{\ln(2/z)-1}{r}\right] + kT\left[\left(\frac{\phi_1}{r_1}\right)(r_1-2)\ln(1-f_1) + \left(\frac{\phi_2}{r_2}\right)(r_2-2)\ln(1-f_2)\right]\right\} \quad (18b)$$

We now consider the special case of a binary mixture of a semiflexible polymer and a small fluid molecule. For the latter, δ/ω is a constant independent of temperature. Denoting the small fluid molecule as component 1, its chemical potential in the pure state $\mu_1°$ is given, to within an additive constant, by the usual lattice fluid expression:

$$\mu_1°/kT = r_1[(-\tilde{\rho}_1 + \tilde{P}_1\tilde{v}_1)/\tilde{T}_1 + (\tilde{v}_1-1)\ln(1-\tilde{\rho}_1) + \ln\tilde{\rho}_1/r_1] \quad (19)$$

In the mixture, the chemical potential μ_1 obtained from the Gibbs potential in the usual way results in the lattice fluid expression:[41]

$$\mu_1/kT = \ln\phi_1 + (1-r_1/r_2)\phi_2 + r_1\tilde{\rho}X_{12}\phi_2^2 + r_1[(-\tilde{\rho} + \tilde{P}_1\tilde{v})/\tilde{T}_1 + (\tilde{v}-1)\ln(1-\tilde{\rho}) + \ln\tilde{\rho}/r_1] \quad (20)$$

Note that eq 19 is obtained from eq 20 by setting $\phi_2 = 0$. The condition of equilibrium between pure fluid and fluid dissolved in the polymer is obtained when $\mu_1° = \mu_1$.

The Gibbs–Di Marzio criterion of the glass transition is based on the hypothesis that an ideal glass transition temperature, T_2, occurs at infinitely slow cooling. At T_2 the polymer essentially becomes "frozen" and has zero entropy.[34] Unfortunately, T_2 cannot be evaluated experimentally; instead T_g is determined for a finite cooling rate. It has been proposed that T_2 is lower than T_g by about 50 °C.[46] If the decrease in entropy is the cause of the glass transition, then it is reasonable to assume that the relation between T_g and entropy should be the same as for T_2 and entropy, with the result $S = 0$ at the experimental T_g. The sorption of the fluid in the polymer and the T_g may be calculated by solving the equation of state, condition of equilibrium, and the Gibbs–Di Marzio criterion simultaneously. In the case of a mixture, it is the mixture entropy that is zero at the T_g, not the entropy of the pure polymer, according to the Gibbs–Di Marzio theory.[35] In the analysis of Conforti et al.,[47] it was assumed that the pure polymer entropy is zero. In the implementation of eq 17b, the fluid diluent is assumed to be fully flexible, unlike the polymer. Mathematically, this is equivalent to setting $\Delta\epsilon_1 = 0$ in eqs 10 and 17b as stated previously.

Results and Discussion

Fundamental Types of Glass Transition Behavior. In this section, we define and characterize fundamental types of T_g versus pressure behavior over a wide range of temperature and pressure, where the fluid may exist as gas, liquid, or supercritical fluid. We examine the behavior as a function of the (1) solubility of the fluid in the liquid polymer, (2) polymer flexibility (likewise the normal T_g), and (3) critical temperature of the fluid. The solubility of a fluid in a polymer is influenced by two primary physical properties, the polymer–fluid interaction strength and the fluid's critical temperature, a measure of its characteristic attraction energy. The influence of T_c on the T_g behavior is complex, since it effects the temperature difference between the normal T_g and the critical region as well as the solubility.

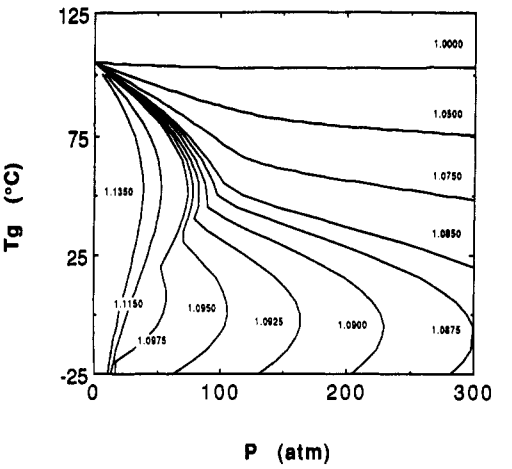

Figure 1. T_g behavior as a function of pressure for various labeled values of the polymer–CO_2 interaction parameter, ζ_{12}. Characteristic pure component parameters are for PMMA and CO_2 and a normal polymer T_g of 105 °C.

Table I
Characteristic Parameters Used in This Study

substance	T^* (K)	P^* (MPa)	ρ^* (kg/m^3)	$\Delta\epsilon_2$ (J/mol)
CO_2	308.64	574	1505	
PMMA	696	503	1269	7443
PS	735	357	1105	7151

Effect of Solubility of the Compressed Fluid. In this section the solubility is manipulated by varying the polymer–fluid interaction strength with the interaction parameter ζ_{12} as shown in eq 9. Because the fluid's T_c is fixed, the location of the normal glass transition temperature ($T_g°$) (i.e., at 1 atm) with respect to the critical point is constant, simplifying the analysis, for reasons which will become clear in subsequent sections. We consider a hypothetical system in which the pure component characteristic parameters (i.e., T^*, P^*, and ρ^*) are those of CO_2 and poly(methyl methacrylate) (PMMA) (see Table I). The calculated T_c (45.9 °C) is larger than the experimental value for CO_2 for the lattice fluid parameters determined in a previous study.[48] The value of $\Delta\epsilon_2$ was regressed by application of eqs 15 and 17b to the case of a pure polymer with $T_g° = 105$ °C for a chosen value of z of 10. As shown in Figure 1, both the nature and the magnitude of the T_g versus pressure behavior are influenced markedly by the strength of this polymer–fluid interaction ζ_{12}. As this interaction becomes stronger, the chemical potential of the fluid in the polymer decreases, thus increasing the solubility and the T_g depression, as shown by the model.

Four distinct fundamental types of T_g versus pressure behavior may be identified in Figure 1 and are reproduced in Figure 2 (see Table II). Type I T_g–pressure behavior is characterized by a T_g minimum. As explained by Wang et al.,[13] who observed this behavior experimentally, the T_g minimum is due to two opposing effects, a diluent effect and a hydrostatic pressure effect. At low pressures, the decrease in T_g is dominated by the increase in solubility with pressure, a diluent effect. The diluent increases the distance between polymer segments, thus decreasing the strength of the inter- and intramolecular interactions between segments. The weakening of these interactions increases the molecular motion, which can lead to a glass to liquid transition. The diluent also increases the free volume available to the polymer segments. At high pressures, the hydrostatic pressure effect is dominant and

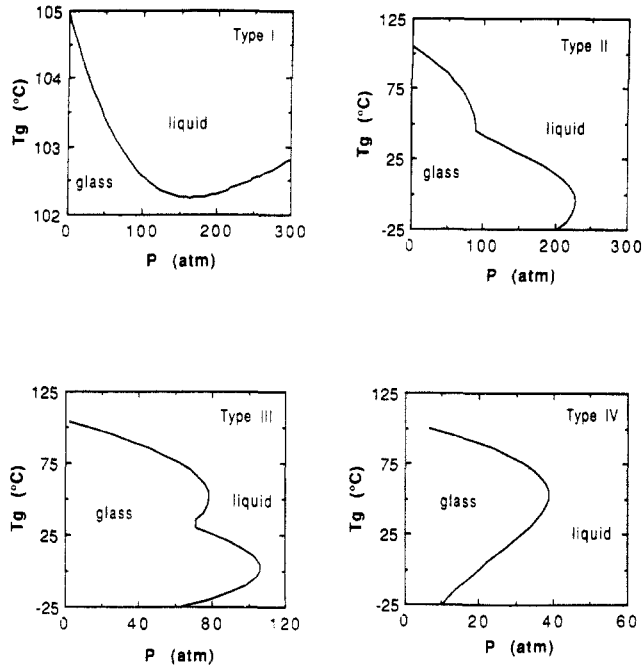

Figure 2. Types of T_g behavior as a function of pressure predicted by the model.

Table II
Definition of Four Fundamental Types of T_g vs Pressure Behavior Predicted by Model

type	T_g–pressure characteristics	T_g–w_1 characteristics
I	T_g minimum	T_g minimum
II	P maximum ($T < T_c$)	linear
III	P maximum ($T > T_c$) P maximum ($T < T_c$)	linear
IV	P maximum ($T > T_c$)	linear

T_g increases. At these pressures, the solubility does not increase significantly with pressure. Here, the hydrostatic pressure decreases the molecular distance between polymer segments (and the free volume), inhibiting both molecular motion and a glass to liquid transition. As is evident in Figure 1, type I behavior is expected for systems in which the solubility of the compressed fluid in the polymer is low (small ζ_{12}).

As the solubility of the fluid in the polymer increases, a pressure maximum in T_g appears, for example, as ζ_{12} increases to 1.0900 in Figure 1. This behavior, which we call type II, is characterized by a single pressure maximum at a temperature below the critical temperature of the compressed fluid (see Figure 2). The discontinuity in the slope of T_g versus pressure occurs on the vapor pressure curve.

An interesting and unusual phenomenon has been discovered with the model, as shown in Figure 2. Consider the type II behavior at 220 atm, starting at 50 °C. As the temperature decreases, the polymer undergoes an expected liquid to glass transition. However, a further decrease causes the glass to again become a liquid! Conversely, an increase in temperature from low temperature causes a liquid to glass transition, opposite the normal behavior. We call this phenomenon retrograde vitrification (by analogy with retrograde condensation). It occurs in regions where the slope of T_g versus pressure is positive.

A further increase in the solubility (described by ζ_{12}) produces type III behavior, which exhibits two pressure maxima. One pressure maximum occurs at a temperature above, and one below, the critical temperature of the compressed fluid. There are two regions with positive slopes which exhibit retrograde vitrification, i.e., liquid to glass transitions with an increase in temperature. At 75 atm, the model predicts four transitions from low temperature to high temperature where the polymer will be a liquid, glass, liquid, glass, and finally a liquid! Type II and III behavior have not yet been observed experimentally.

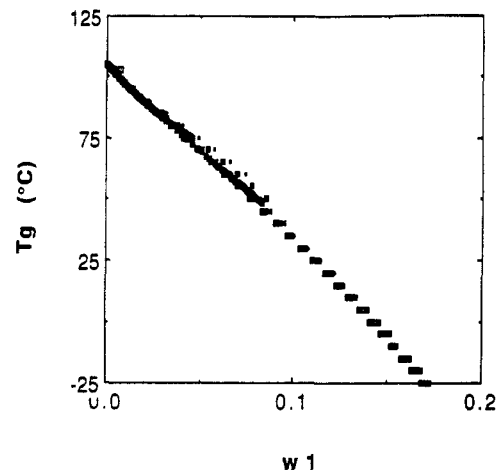

Figure 3. T_g behavior as a function of solubility (weight fraction units) of the compressed fluid in the polymer. Results include all ζ_{12} and T_1^* values in Figures 1 and 8.

For the highest solubilities in Figure 1, type IV T_g–pressure behavior is observed which exhibits a single pressure maximum at temperatures above the critical temperature of the compressed fluid. Retrograde vitrification is present at temperatures below about 50 °C where the slope becomes positive. Although very few data have been reported in this region, there is experimental evidence to support this type of behavior, as explained in the second part of this study.

Despite the varied and complex nature of the four fundamental types of T_g versus pressure behavior, the analogous T_g versus sorption behavior is simple and relatively linear (Figure 3). Indeed all of the curves in Figure 1 collapse to a single line. This simple near-linear prediction of the model has been observed experimentally and can be related to phenomenological models used to describe T_g behavior.[49] According to Figure 3, for a constant temperature decrease, a constant sorption increase is needed to produce a glass transition. In essence, the T_g depression is governed simply by the sorption. The question then is: What pressure at a given temperature is needed to obtain the sorption required to produce a glass to liquid transition of the polymer? Asked another way, what are the effects of temperature and pressure on the solubility behavior of the compressed fluid in the polymer? The answer to these questions will explain the complex T_g versus pressure behavior, including the retrograde vitrification phenomenon.

The solubilities of compressed fluids in polymers are most often reported as isotherms. Figure 4 shows isotherms generated by the model over a more extended temperature and pressure range than usually reported in the literature. Below the critical temperature, there is a discontinuity in the slope of sorption versus pressure which falls on the vapor pressure curve as expected. At pressures less than the vapor pressure, the fluid is a gas and the slope of sorption versus pressure is relatively large. At high pressures above the vapor pressure where the fluid is a liquid, the slope is relatively small. Above the critical temperature, the change from vapor-like to liquid-like sorption behavior is still present but occurs over a broader pressure range and without a phase change. As temper-

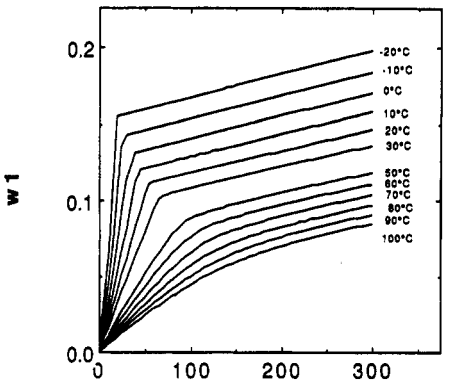

Figure 4. Theoretical sorption isotherms versus pressure (ζ_{12} = 1.0950; characteristic parameters for PMMA and CO_2).

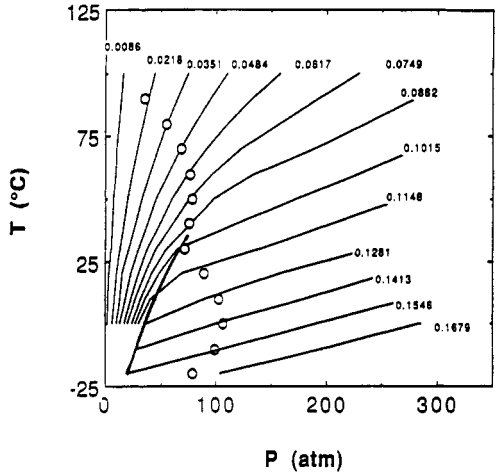

Figure 5. Theoretical sorption isopleths for the conditions in Figure 4 (labeled values are in units of weight fraction): (O) predicted T_g values with a polymer normal T_g = 105 °C; (—) vapor pressure curve for CO_2.

ature is increased far above the critical temperature, the transition between vapor- and liquid-like regions is indistinguishable. The combination of the complex pressure and temperature effects on the sorption, particularly near the critical point of the fluid, is the cause of the fascinating four types of T_g versus pressure behavior, including retrograde vitrification.

It is easier to visualize the cause of retrograde T_g–pressure behavior by examining sorption isopleths, as shown in Figure 5. The sorption isopleths were calculated for the most complex type of behavior, type III (ζ_{12} = 1.0950). The increment in each adjacent pair of isopleths is chosen to be constant (0.0132), to correspond to a change in T_g of 10 °C based on the linear behavior of T_g versus sorption in Figure 3. As was the case for the isotherms in Figure 4, the slopes of the isopleths are quite different at pressures above and below the vapor pressure curve. At a given temperature, the sorption is sensitive to pressure in the gaseous region; i.e., the isopleths are closely spaced. The opposite is observed in the liquid region. For a fluid just above the critical point, the behavior is highly variable as the fluid changes from gas-like to liquid-like conditions. The next step is to examine how these features influence the T_g versus pressure behavior.

The cause of the pressure maxima in T_g versus pressure, and, likewise, the retrograde vitrification behavior, becomes apparent by the following illustration. We begin by plotting the T_g at 90 °C which falls on the 0.0218 isopleth. Next, the temperature is decreased 10 °C. The sorption must change to the next isopleth, since they were constructed to correspond to 10 °C changes as discussed above. For this step to 80 °C, the next isopleth is at a higher pressure. However, for the step from the 0.0749 to 0.0882 isopleth (50 to 40 °C), the pressure actually decreases, indicating a retrograde region. This pressure decrease also takes place for the next step and for the last two steps at the lowest temperatures. This exercise illustrates that it is the balance between temperature and pressure effects on sorption which determines whether or not a system is in the retrograde region. The normal behavior is encountered in the fluid phase well above the critical temperature, but the retrograde behavior appears closer to the critical point where there are complex changes in the sorption isopleths with temperature and pressure.

The features of the other types of T_g behavior may also be explained in terms of isopleths. As the fluid–polymer interactions become stronger, the numerical values of the isopleths will increase, but the shapes will be similar since the vapor pressure curve and critical point of the fluid are fixed. For type IV behavior, solubilities are sufficiently high that none of the isopleths intersect the vapor pressure curve over the temperature range of interest. Here a fluid is sufficiently soluble to cause large T_g depressions at relatively low pressures. A pressure maximum is produced since the isopleths are closer together as temperature is decreased in this region. In the case of type II behavior, the solubility of the fluid in the polymer is relatively low; thus higher pressures are needed to achieve the sorption required for a glass transition.

The complex temperature and pressure effects on the T_g–pressure behavior may be shown with the phase equilibrium criterion[50]

$$-\left[\frac{(\bar{h}_1^{\,P} - \bar{h}_1^{\,F})}{RT^2}\right] dT + \left[\frac{(\bar{v}_1^{\,P} - \bar{v}_1^{\,F})}{RT}\right] dP + \left(\frac{\partial \ln f_1^{\,P}}{\partial w_1^{\,P}}\right)_{T,P} dw_1^{\,P} = 0 \quad (21)$$

where $\bar{h}_1^{\,P}$ is the partial molar enthalpy of the diluent in the polymer phase, $\bar{v}_1^{\,P}$ is the partial molar volume, $f_1^{\,P}$ is the fugacity, $w_1^{\,P}$ is the weight fraction and likewise in the fluid phase. This equation has been simplified by the condition that the polymer is insoluble in the fluid phase. On the basis of the result in Figure 3, we assume

$$dw_1^{\,P} = -A\, dT_g^{\,P} \quad (22)$$

where A is a positive constant. Thus, the slope of T_g versus P may be written as

$$\frac{\partial T_g}{\partial P} = \frac{\dfrac{\bar{v}_1^{\,P} - \bar{v}_1^{\,F}}{RT_g}}{\dfrac{\bar{h}_1^{\,P} - \bar{h}_1^{\,F}}{RT_g^{\,2}} + A\left(\dfrac{\partial \ln f_1^{\,P}}{\partial w_1^{\,P}}\right)_{T_g,P}} \quad (23)$$

At high T where the fluid volume is large, $\bar{v}_1^{\,P} < \bar{v}_1^{\,F}$; therefore the numerator is negative. In the denominator, $\bar{h}_1^{\,P} < \bar{h}_1^{\,F}$ (e.g., the enthalpy of vaporization is positive) so that the first term is negative and $\partial f_1^{\,F}/\partial w_1^{\,F}$ is positive from stability. The second term in the denominator must dominate since $\partial T_g/\partial P$ is negative. At low T, $\partial T_g/\partial P$ can be positive. Both $\bar{v}_1^{\,P} - \bar{v}_1^{\,F}$ and $\bar{h}_1^{\,P} - \bar{h}_1^{\,F}$ can undergo a sign change[7] (e.g., which leads to retrograde temperature and pressure effects on the solubilities of solids in fluids[51,52]). Again, the sign change in $\partial T_g/\partial P$ is caused by

Table III
Flex Energy Calculated as a Function of the Normal Glass Transition Temperature, $T_g°$ [a]

$T_g°$ (K)	$\Delta\epsilon_2$ (J/mol)	$T_g°$ (K)	$\Delta\epsilon_2$ (J/mol)
348.15	10671	423.15	13517
378.15	11783	473.15	15536
398.15	12544		

[a] T_2^* = 696 K, P_2^* = 503 MPa, ρ_2^* = 1269 kg/m^3, ζ_{12} = 1.0950, z = 10.

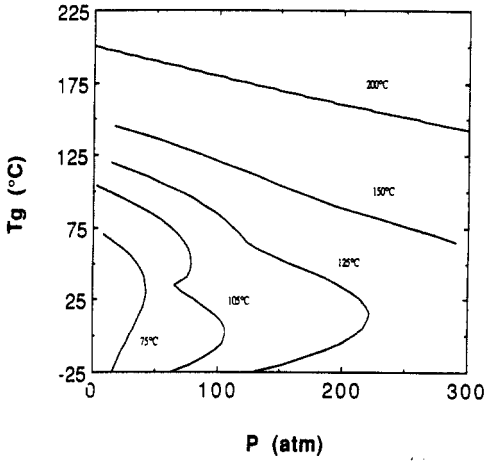

Figure 6. Predicted T_g behavior as a function of pressure for various labeled $T_g°$ values (ζ_{12} = 1.0950; characteristic parameters for PMMA and CO_2).

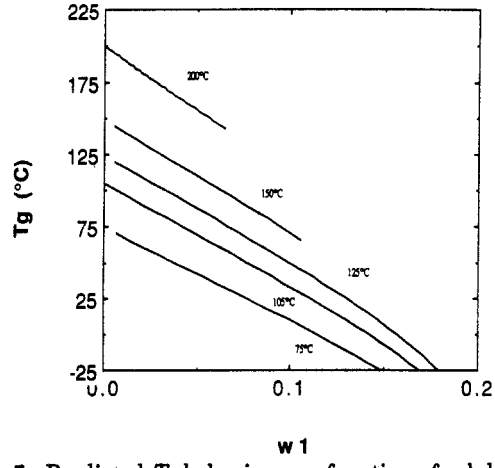

Figure 7. Predicted T_g behavior as a function of solubility of the compressed fluid in the polymer for conditions in Figure 6.

the complex pressure and temperature effects on sorption.

Effect of the Polymer Flexibility. To study the effect of the flexibility of the polymer, the normal glass transition temperature, $T_g°$, is varied while holding all other parameters constant (see Table III). Varying $T_g°$ varies the flex energy of the polymer, $\Delta\epsilon_2$. The resulting T_g behavior is shown in Figure 6 for five different $T_g°$ values. Three of the four types of T_g–pressure behavior are observed. Type I behavior is expected for polymers with values of $T_g°$ above 125 °C, but it has not yet been determined what $T_g°$ is required. Figure 7 shows that the T_g–sorption characteristics are nearly linear for all $T_g°$ values and that the slopes are quite similar. That is, the sorption increase needed for a given glass transition temperature depression is the same regardless of the $T_g°$ of the polymer. Again, the T_g depression is dictated by the solubility behavior.

Because the flex energy does not affect the solubilities, the isopleths are exactly the same as in Figure 5. For Figure 5, where $T_g°$ = 105 °C, we showed the behavior is type III. For a $T_g°$ of 75 °C, the T_g versus pressure path always stays on isopleths at pressures below the vapor pressure curve, i.e., in the gas-phase region (Type IV), as shown in Figure 6. For a $T_g°$ of 125 °C, considerably higher pressures are needed to depress the T_g to 25 °C. The pressure trace enters a region with liquid-like sorption isopleths and type II behavior is observed. For the 150 and 200 °C $T_g°$ values, the isopleths are sufficiently far from the critical point that T_g is nearly linear for the pressure range studied. In summary, the behavior varies from type II to type IV behavior as the difference between $T_g°$ and the critical temperature decreases.

Table IV
Parameters Used To Study the Effect of the Fluid Critical Temperature on the T_g Behavior[a]

T_1^* (K)	T_c (K)	P_c (MPa)
248.00	271.95	7.17
283.00	299.65	8.33
300.00	312.55	8.89
305.00	316.35	9.06
308.64	319.05	9.18
350.00	348.95	10.54

[a] P_1^* and ρ_1^* are for CO_2 in Table I.

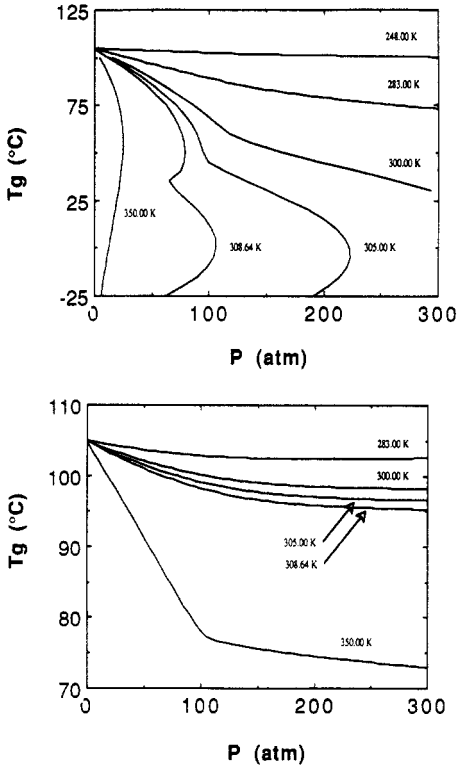

Figure 8. Predicted T_g behavior as a function of pressure for various values of the diluent characteristic temperature, T_1^*: (a, top) ζ_{12} = 1.0950; (b, bottom) ζ_{12} = 1.0000.

Effect of the Critical Temperature of the Compressed Fluid. The behavior of T_g is influenced by the critical temperature of the fluid, T_c, for two primary reasons. As T_c increases, solubility increases and, consequently, the T_g depression. Also, the difference between $T_g°$ and T_c varies, which also has a large effect on the behavior as shown in the previous section.

In this section T_c is varied while holding most of the remaining properties constant, e.g., ζ_{12}, z, and $\Delta\epsilon_2$. Since the critical density is constant, the critical pressure varies. The T_c is related directly to the characteristic temperature in lattice fluid theory, T_1^*, as shown in Table IV. Results are presented for two different values of ζ_{12} in Figure 8. Again, the T_g–sorption behavior falls on the same curve shown in Figure 3. Consider the case where ζ_{12} = 1.0950. As T_1^* increases, the solubility increases, driving the

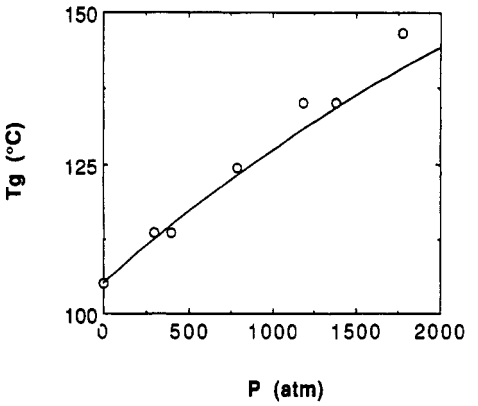

Figure 9. T_g behavior as a function of pressure for pure PMMA: (—) correlated; (O) Olabisi and Simha.[53]

system from type I to type IV as in Figure 8a. Simultaneously, the T_c becomes closer to $T_g°$ and the isopleths remain more in the vapor-like region as discussed in detail in the previous section. The system moves from type I to II to III to IV behavior. This change in behavior is reinforced in a synergistic manner by the increased solubilities. As T_1* decreases from 308.64 to 305 K, T_c moves further from $T_g°$ and larger pressures are required to depress T_g to the critical temperature. The T_g versus pressure trace traverses the vapor-like isopleth region and enters the liquid-like region, producing type III behavior.

For $\zeta_{12} = 1.0$ the solubility of the compressed fluid is low relative to the $\zeta_{12} = 1.0950$ value. Larger pressures are required to depress the T_g; thus the T_g versus pressure curves do not come close to the critical region.

Comparison of the Model with Experiment. Pure Poly(methyl methacrylate) (PMMA). We begin by comparing the correlation of the model with experimental data for the hydrostatic pressure effect on pure PMMA without a diluent. The data used to regress z and $\Delta\epsilon_2$ simultaneously are the normal glass transition temperature ($T_g°$) (i.e., 1 atm) and the dT_g/dP of the pure polymer.[53,54] Only whole numbers were considered for possible values of z and the regressed value was $z = 5$. Equations 15 and 17b for the case of a pure polymer were used in the regression. The results in Figure 9 are very good over most of the pressure range studied and show a finite asymptote at high pressures. It has been shown that the Gibbs–Di Marzio criterion yields such a result.[46] The calculation for PS yielded results similar to a previous study,[55] and again, $z = 5$.

PMMA–CO_2 and PS–CO_2 Systems. To apply the model to a real polymer–compressed fluid system, it is necessary to correlate the interaction strength between the polymer and fluid. The binary energy interaction parameter, ζ_{12}, is correlated only at conditions corresponding to a liquid polymer, since glassy polymers are not at equilibrium. Figures 10 and 11 show the results of the correlation for the solubility of CO_2 in PMMA and PS.[56,57] In the case of PMMA this means a total of seven points were used in the correlation in the liquid region. In the case of PS only two points were available. It is noted that no T_g data are used in correlating ζ_{12} from sorption data. Both the data and model indicate a sharp decrease in the slope of the sorption isotherms at conditions near the critical point of the compressed fluid. The characteristic parameters used for CO_2 give a critical temperature which is too high, leading to these discontinuities, which are due to the vapor pressure curve. The model is also able to predict the sorption of the CO_2 in the glassy region without the use of any order parameters, but this could be fortuitous for these data. In general, the glassy sorption

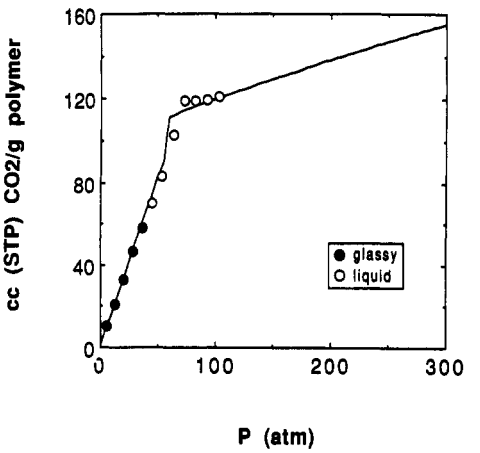

Figure 10. Solubility of CO_2 in PMMA at 32.7 °C ($\zeta_{12} = 1.1350$): (—) correlated; (O; ●) Wissinger and Paulaitis.[56,57]

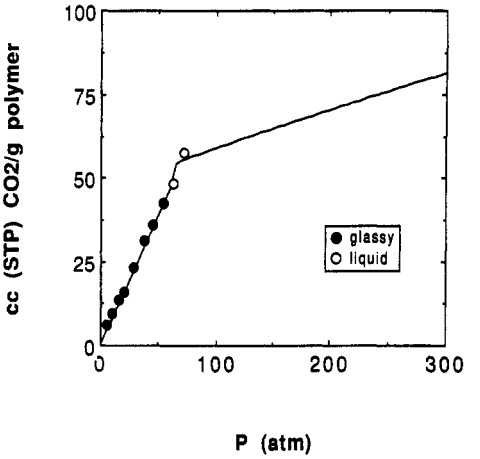

Figure 11. Solubility of CO_2 in PS at 35.0 °C ($\zeta_{12} = 1.1240$): (—) correlated; (O, ●) Wissinger and Paulaitis.[56,57]

region is characterized by an isotherm that is concave to the pressure axis due to the filling of holes at low pressure,[58] which the model does not consider in its present form.

Two computational schemes were used to calculate the glass transition point (i.e., T_g and P_g) simply as a matter of convenience because of the extrema present in the T_g versus pressure relationship. The calculations always started in the equilibrium liquid region where the model is applicable. Either the pressure was held constant and the temperature varied or the temperature was held constant and the pressure varied to reach the glass transition. The former technique is more appropriate for the systems with a temperature minimum, and the latter for those with a pressure maximum. Figures 12 and 13 show the results for the prediction of T_g versus sorption for the PMMA–CO_2 and PS–CO_2 systems. The flexibility of the polymer molecule is characterized by the coordination number z and the flex energy term $\Delta\epsilon_2$ which are calculated from the normal glass transition temperature and the dT_g/dP behavior of the pure polymer and listed in Table I. Very good agreement is observed between the model prediction and the experimental data. All of the newer models discussed in this work use a correlation requiring some equilibrium data, e.g., sorption data, to characterize the polymer–compressed fluid interaction parameter. The difference in the models is in the definition and application of the glass transition criterion. The only other information used in this model to predict the glass transition of the polymer is the normal glass transition temperature and the dT_g/dP behavior of the pure polymer. The other models require considerably more extensive experimental data to calculate the T_g. The normal glass

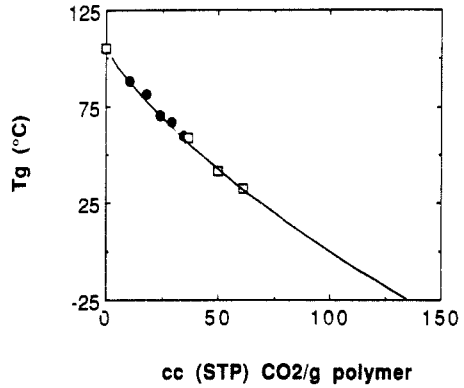

Figure 12. T_g depression of PMMA as a function of solubility of CO_2 in the polymer: (—) predicted; (•) Chiou et al.[14]; (□) Wissinger and Paulaitis.[16]

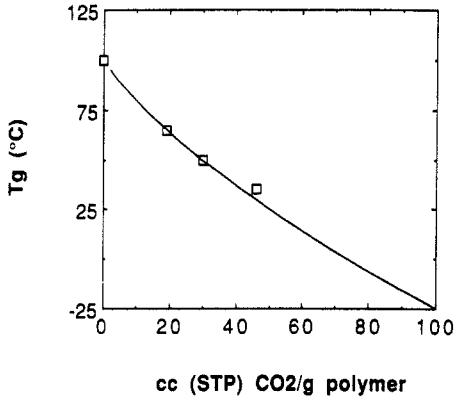

Figure 13. T_g depression of PS as a function of solubility of CO_2 in the polymer: (—) predicted; (□) Wissinger and Paulaitis.[16]

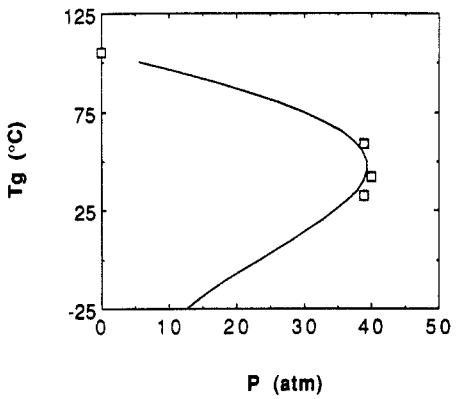

Figure 14. T_g depression of PMMA as a function of CO_2 pressure in the PMMA–CO_2 system: (—) predicted; (□) Wissinger and Paulaitis.[16]

transition temperature of the pure polymer is known for most polymers or can be obtained readily by the well-established DSC technique. In one reference[59] the dT_g/dP behavior of a pure polymer has been approximated as a universal constant of 0.025 °C/bar from data showing a variation from 0.016 to 0.031 °C/bar.[60]

In Figures 14 and 15 T_g versus pressure behavior is predicted and compared with experiment. The predictions exhibit type IV T_g–pressure behavior, which is characterized by a pressure maximum above the critical temperature of the fluid as stated earlier. The experimental data for the PMMA–CO_2 system show an initial negative slope followed by a nearly infinite slope close to the critical point. Although the possibility of retrograde vitrification for these data has not been raised previously, it clearly exists, especially after observing the predictions of the model. The predictions of the model are in qualitative,

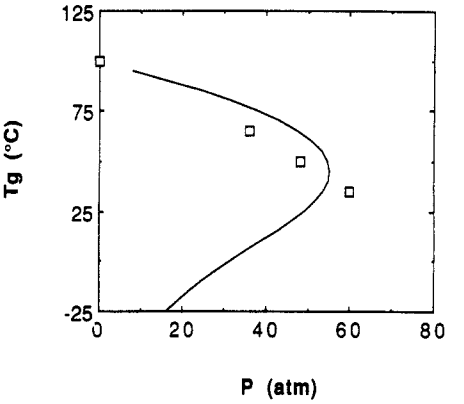

Figure 15. T_g depression of PS as a function of CO_2 pressure in the PS–CO_2 system: (—) predicted; (□) Wissinger and Paulaitis.[16]

if not quantitative, agreement with experiment. Although the PMMA data support the model predictions, there are not enough data for the PS system to test the model.

Conclusions

The model describes accurately equation of state properties, phase equilibria, and the glass transition in a consistent manner over a very broad range in pressure and temperature. In general, the model is applicable to pressurized as well as unpressurized systems and to polymer, gas, liquid, and supercritical fluid diluents. An important advantage over earlier models is that minimal information about the nature of the pure glassy polymer is required, that is the normal T_g and the T_g versus pressure behavior of the pure polymer, which are used to determine the flex energy and the coordination number.

Four distinct fundamental types of T_g versus pressure diagrams are identified as a function of three primary factors: the solubility of the compressed fluid in the polymer, the flexibility of the polymer molecule, and the critical temperature of the fluid. The complex types of T_g versus pressure behavior collapse onto a simple nearly linear curve when the T_g is plotted as a function of the sorption of the fluid in the polymer. For a given T_g, a certain pressure is required to achieve the necessary sorption. This pressure decreases as the polymer–fluid interactions become stronger or the T_c of the fluid increases. This causes the behavior to evolve from type I to type IV. This change in behavior also occurs as the difference between the normal T_g of the polymer and T_c of the fluid diminishes.

A new phenomenon, which we call retrograde vitrification, is a consequence of the complex effects of temperature and pressure on sorption. In this retrograde region at constant pressure, sorption increases markedly with a reduction in temperature, thus causing a glass to liquid transition. If the phenomenon of retrograde vitrification can be confirmed experimentally, then polymers may be plasticized with compressed fluids under much milder conditions than presently believed.

For the limited data which are available for the polystyrene–CO_2 and poly(methyl methacrylate)–CO_2 systems, the predictions of the model are in good agreement with experiment. Although the data provide limited support for type IV T_g versus pressure behavior, a great deal of additional data are required to further judge the predictions of the model. The general characterization of types of T_g behavior should serve as a useful guide for experimental design.

Acknowledgment. Acknowledgment is made to the Separations Research Program at The University of Texas,

the State of Texas Energy Research in Applications Program, and the Camille and Henry Dreyfus Foundation for a Teacher–Scholar Grant (to K.P.J.). Financial support for this work has also been provided by the Air Force Office of Scientific Research and the National Science Foundation (I.C.S. and C.G.P.).

References and Notes

(1) McHugh, M. A.; Krukonis, V. J. *Supercritical Fluid Extraction: Principles and Practice*; Butterworths: Boston, 1986.
(2) McHugh, M. A.; Krukonis, V. J. *Encyclopedia of Polymer Science and Technology*; Mark, H. F., Bikales, N. M., Overberger, C. G., Menges, G., Eds.; Wiley-Interscience: New York, 1989; Vol. 16, p 368.
(3) Ehrlich, P. *Chemtracts—Macromol. Chem.* **1992**, *3*, 1.
(4) Daneshvar, M.; Gulari, E. *Supercritical Fluid Science and Technology*; Johnston, K. P., Penninger, J. M. L., Eds.; ACS Symposium Series 406; American Chemical Society: Washington, DC, 1989.
(5) Kiran, E.; Saraf, V. P.; Sen, Y. L. *Int. J. Thermophys.* **1989**, *10*, 437.
(6) Shim, J.-J.; Johnston, K. P. *AIChE J.* **1989**, *35*, 1097.
(7) Shim. J.-J.; Johnston, K. P. *J. Phys. Chem.* **1991**, *95*, 353.
(8) Shim. J.-J.; Johnston, K. P. *AIChE J.* **1991**, *37*, 607.
(9) Seckner, A. J.; McClellan, A. K.; McHugh, M. A. *AICHE J.* **1988**, *34*, 9.
(10) Watkins, J. J.; Krukonis, V. J.; Condo, P. D.; Pradhan, D.; Ehrlich, P. *J. Supercrit. Fluids* **1991**, *4*, 24.
(11) Meilchen, M. A.; Hasch, B. M.; McHugh, M. A. *Macromolecules* **1991**, *24*, 4874.
(12) Chen, S. J.; Radosz, M. *2nd Int. Symp. Supercrit. Fluids, Proc.* **1991**, *225*.
(13) Wang, W.-C. V.; Kramer, E. J.; Sachse, W. H. *J. Polym. Sci., Polym. Phys. Ed.* **1982**, *20*, 1371.
(14) Chiou, J. S.; Barlow, J. W.; Paul, D. R. *J. Appl. Polym. Sci.* **1985**, *30*, 2633.
(15) Hachisuka, H.; Sato, T.; Imai, T.; Tsujita, Y.; Takizawa, A.; Kinoshita, T. *Polym. J.* **1990**, *22*, 77.
(16) Wissinger, R. G.; Paulaitis, M. E. *J. Polym. Sci., Part B: Polym. Phys.* **1991**, *29*, 631.
(17) Kamiya, Y.; Mizoguchi, K.; Hirose, T.; Naito, Y. *J. Polym. Sci., Part B: Polym. Phys.* **1989**, *27*, 879.
(18) Briscoe, B. J.; Zakaria, S. *J. Polym. Sci., Part B: Polym. Phys.* **1991**, *29*, 989.
(19) Garg, A.; Gerhardt, L.; Gulari, E.; Manke, C. W. *2nd Int. Symp. Supercrit. Fluids, Proc.* **1991**, *225*.
(20) Pope, D. S.; Koros, W. J. *Macromolecules* **1992**, *25*, 1711.
(21) Kumar, V.; Suh, N. P. *Polym. Eng. Sci.* **1990**, *30*, 1323.
(22) Lele, A. K.; Shine, A. D. *AIChE J.* **1991**, *38*, 742.
(23) Tom, J. W.; Debenedetti, P. G. *Biotechnol. Prog.* **1991**, *7*, 403.
(24) Tom, J. W.; Debenedetti, P. G. *J. Aerosol Sci.* **1991**, *22*, 555.
(25) Dixon, D. J.; Johnston, K. P., submitted to *AIChE J.*
(26) Matson, D. W.; Fulton, J. L.; Petersen, R. C.; Smith, R. D. *Ind. Eng. Chem. Res.* **1987**, *26*, 2298.
(27) Matson, D. W.; Fulton, J. L.; Petersen, R. C.; Smith, R. D. *Polym. Eng. Sci.* **1987**, *27*, 1693.
(28) Bush, P. J.; Pradhan, D.; Ehrlich, P. *Macromolecules* **1991**, *24*, 1439.
(29) Pradhan, D.; Stewart, R. B.; Gebo, T. E.; Ehrlich, P. *2nd Int. Symp. Supercrit. Fluids, Proc.* **1991**, *225*.
(30) Lee, C.; Hoy, K. L.; Donohue, M. D. U.S. Patent 4,923,720, 1990.
(31) Hoy, K. L.; Donohue, M. D. *ACS Prepr.* **1990**, 679.
(32) Assink, R. A. *J. Polym. Sci., Polym. Phys. Ed.* **1974**, *12*, 2281.
(33) Chow, T. S. *Macromolecules* **1980**, *13*, 362.
(34) Gibbs, J. H.; Di Marzio, E. A. *J. Chem. Phys.* **1958**, *28*, 373.
(35) Di Marzio, E. A.; Gibbs, J. H. *J. Polym. Sci., Part A* **1963**, *1*, 1417.
(36) Beckman, E. J. Ph.D. Dissertation, University of Massachusetts at Amherst, Amherst, MA, 1988.
(37) Beckman, E. J.; Porter, R. S.; Koningsveld, R. *Polym. Prepr. (Am. Chem. Soc., Div. Polym. Chem.)* **1989**, *30*, 683.
(38) Wissinger, R. G.; Paulaitis, M. E. *Ind. Eng. Chem. Res.* **1991**, *30*, 842.
(39) Kalospiros, N. S.; Astarita, G.; Paulaitis, M. E. Presented at the AIChE meeting in Los Angeles, November 1991.
(40) Sanchez, I. C.; Lacombe, R. H. *J. Phys. Chem.* **1976**, *80*, 2352.
(41) Sanchez, I. C.; Lacombe, R. H. *Macromolecules* **1978**, *11*, 1145.
(42) Panayiotou, C. G. *Makromol. Chem.* **1986**, *187*, 2867.
(43) Panayiotou, C. G. *Macromolecules* **1987**, *20*, 861.
(44) Flory, P. J. *Proc. R. Soc. London, Ser. A* **1956**, *234*, 60.
(45) Panayiotou, C. G. *Polym. J.* **1986**, *18*, 895.
(46) Di Marzio, E. A.; Gibbs, J. H.; Fleming, P. D.; Sanchez, I. C. *Macromolecules* **1976**, *9*, 763.
(47) Conforti, R. M.; Barbari, T. A.; Vimalchand, P.; Donohue, M. D. *Macromolecules* **1991**, *24*, 3388.
(48) Panayiotou, C.; Sanchez, I. C. *Polym. Commun.*, in press.
(49) Gordon, J. M.; Rouse, G. B.; Gibbs, J. H.; Risen, W. M. *J. Chem. Phys.* **1977**, *66*, 4971.
(50) Modell, M.; Reid, R. C. *Thermodynamics and Its Applications*; Prentice-Hall: Englewood Cliffs, NJ, 1983.
(51) Chimowitz, E. H.; Pennisi, K. J. *AIChE J.* **1986**, *32*, 1665.
(52) Johnston, K. P.; Barry, S. E.; Read, N. K.; Holcomb, T. R. *Ind. Eng. Chem. Res.* **1987**, *26*, 2372.
(53) Olabisi, O.; Simha, R. *Macromolecules* **1975**, *8*, 204.
(54) Quach, A.; Simha, R. *J. Appl. Phys.* **1971**, *42*, 4592.
(55) Panayiotou, C.; Vera, J. H. *J. Polym. Sci., Polym. Lett. Ed.* **1984**, *22*, 601.
(56) Wissinger, R. G.; Paulaitis, M. E. *J. Polym. Sci., Part B: Polym. Phys.* **1987**, *25*, 2497.
(57) Wissinger, R. G. Ph.D. Dissertation, University of Delaware, Newark, DE, 1988.
(58) Chiou, J. S.; Maeda, Y.; Paul, D. R. *J. Appl. Polym. Sci.* **1985**, *30*, 4019.
(59) Peyser, P. *Polymer Handbook*; Brandrup, J., Immergut, E. H., Eds.; Wiley-Interscience: New York, 1989.
(60) Shen, M. C.; Eisenberg, A. *Rubber Chem. Technol.* **1970**, *43*, 95.